Canonical variations on the Kob-Andersen model

2002 J. Phys.: Condens. Matter 14 1455

(http://iopscience.iop.org/0953-8984/14/7/305)

INSTITUTE OF PHYSICS PUBLISHING JOURNAL OF PHYSICS: CONDENSED MATTER

J. Phys.: Condens. Matter **14** (2002) 1455–1472 PII: S0953-8984(02)32774-7

Canonical variations on the Kob–Andersen model

Mauro Sellitto

The Abdus Salam International Centre for Theoretical Physics, Strada Costiera 11, PO Box 586, I-34100 Trieste, Italy

Received 18 December 2001
Published 7 February 2002
Online at stacks.iop.org/JPhysCM/14/1455

Abstract

Versions of a lattice-gas model with kinetic constraints have been introduced to address some problems in the physics of slowly relaxing systems, such as the nature of the glass transition, the existence of a probability measure underlying the aging dynamics and non-linear transport in the non-equilibrium steady state. A short review of recent progress is given.

1. Introduction

One of the main problems in the physics of glassy systems is the identification of the microscopic mechanisms leading to slow dynamics and their relationship with a possible underlying thermodynamic phase transition. The ubiquity of glassy behaviour in condensed matter seems to suggest the existence of a certain degree of universality in slow relaxation phenomena. Nevertheless, the fact that glassy behaviour is first of all a kinetic (finite-observation-time) effect makes the glass transition problem far from trivial, from both a computational and an experimental point of view.

The problem is conceptually important because (i) the glass state could be a new *thermodynamic* phase of matter (as in the simpler case of crystals, liquid crystals etc) and (ii) it is related to the possibility of having dynamic ergodicity breaking without a corresponding equilibrium phase transition. On the other hand, it also has very practical interest because—irrespective of the nature of the glass transition—one would ultimately like to be able to predict the behaviour of a sample without needing to know too many details about its history.

In statistical mechanics it is well known that the notion of thermal equilibrium requires a wide timescale separation between 'fast' and 'slow' processes [1], and that it would be useless if the observation time were too large [2]. When such a separation is possible, the macroscopic properties of a body can be obtained by standard techniques of equilibrium statistical mechanics. Emblematic in this respect is the solution to the puzzle of the heat capacity of hydrogen [3]. Many substances we are used to dealing with have macroscopic properties that change relatively quickly with the observation time: they appear solid-like on a short timescale and liquid-like on a longer timescale, a difference which is conveniently described in rheology through the Deborah number (relaxation time/observation time) [4,5]. Depending on our purpose the 'observation time' can be very long: basalt is a liquid for the purpose of

studying continental drift[1]. When the relaxation time increases with the time elapsed since the preparation of the substance, the Deborah number acquires a further *age* dependence: the older the system, the longer it takes to relax. A typical and well documented example is polymeric plastic [6]. One can also mention amorphous magnets [7], and many other systems. The non-equilibrium nature of these materials makes them a challenging object of study for statistical mechanics as there is no apparent form of ergodicity underlying their dynamic evolution. This justifies the use of abstract models which, while reproducing the qualitative behaviour of more realistic systems, may offer a deeper insight into the microscopic nature of relaxation processes and the basic questions related to the formulation of a thermodynamic approach.

1.1. Kinetic constraints

Since its first appearance, the nature of the singularity predicted by the mode-coupling theory [8–11] has been much debated [12, 13]. Mean-field disordered models of structural glasses show that the divergence of the relaxation time occurring at the glass transition is associated with a dynamic transition whose origin is the existence of an extensive entropy of metastable states [14,15]. On the other hand, it is usually argued that the lifetime of metastable states in finite-dimensional short-range models cannot be infinite, since it is always possible to nucleate a droplet of the stable phase by a thermally activated process. Therefore the dynamic transition would be an artifact of the mean-field approximation, and in real glasses it would be smeared out. The glassy behaviour should therefore be a more profound reflection of an underlying complex free-energy landscape due to a non-trivial Gibbs measure. The universality of this scenario can be explored by considering models which are finite dimensional (non-mean-field) and do not contain any disorder or frustration in their Hamiltonian.

A generic microscopic mechanism leading to slow relaxation was introduced some time ago by Fredrickson and Andersen [16], with the purpose of describing the cooperative behaviour in highly viscous liquids. It is based on kinetic rules that allow only a selection of the possible configuration changes but are compatible with detailed balance and the Boltzmann distribution. A kinetic constraint can be so effective that there is no need to introduce a specific energetic interaction between spins. Further, in analogy with mean-field spin-glasses [38], kinetic constraints lead to an extensive entropy of blocked configurations, which is the ultimate reason for the slowing down of the dynamics. Blocked configurations or metastable states are thought of here as configurations in which every spin (particle) is unable to flip (move). Models with such kinetic constraints have been the subject of a considerable number of studies, since they provide a schematic description of the dynamics of strong and fragile glasses [17–30]. One reason for the interest in these models is that some of them appear to have ergodic–nonergodic transitions of the kind predicted by mode-coupling theory. They can therefore be useful for understanding whether the glass transition may have, at least in principle, a purely dynamical nature.

In this respect, it is worth distinguishing excluded-volume effects and kinetic constraints. Excluded-volume effects occur in sterically hindered systems and correspond to the existence of forbidden *states* in the configuration space of the system. For some values of thermodynamic parameters (density, temperature) the geometry of the configuration space can induce an unusual phase behaviour. In fact, peculiar equilibrium transitions take place in hard-core systems, the most famous being the isotropic–nematic transition in three-dimensional systems of thin hard rods [31] (and the most controversial being the freezing of hard spheres). They are generally known as entropy-driven phase transitions since the entropy of the system *increases* in the ordering process [32]. Kinetic constraints are different. They are non-holonomic and correspond to forbidden *transitions* in configuration space. However, even if the Hamiltonian

[1] I owe this example to Luca Peliti.

of a system with kinetic constraint is trivial, the detailed balance condition does not guarantee that such is its Gibbs measure. The *convergence* to the equilibrium measure is guaranteed by the irreducibility of the Markov chain associated with the dynamic evolution. A Markov chain is said to be irreducible if for every pair of configurations $\mathcal{C}$ and $\mathcal{C}'$, either the transition probability $\mathcal{W}(\mathcal{C}, \mathcal{C}')$ is non-zero, or there is some set of intermediate configurations $\mathcal{C}_1, \ldots, \mathcal{C}_n$, such that $\mathcal{W}(\mathcal{C}, \mathcal{C}_1)$, $\mathcal{W}(\mathcal{C}_1, \mathcal{C}_2), \ldots, \mathcal{W}(\mathcal{C}_{n-1}, \mathcal{C}_n)$, $\mathcal{W}(\mathcal{C}_n, \mathcal{C}')$ are all non-zero. In other words, irreducibility means that any state (except for a zero-measure set in the thermodynamic limit) is in principle accessible from any other one, while reducibility means that the configuration space can be partitioned into sets such that the system can never get out of a set if its initial configuration was inside that set.

The two kinds of constraint may ultimately have similar effects, such as very slow dynamics due e.g. to a vanishing transport coefficient, but their microscopic interpretation may be rather different.

The rest of the paper is organized as follows. In section 2 we introduce the Kob–Andersen (KA) model in its original version. When particle exchange with a reservoir is allowed the model is able to reproduce qualitatively many dynamic features of a class of mean-field disordered systems thought to mimic the behaviour of real glasses. These include history dependence, irreversibility effects, power-law approach to the asymptotic state, physical aging, chaoticity and an effective temperature derived from fluctuation–dissipation relations. In section 3 we present numerical support for the hypothesis that macroscopic observables in the aging regime can be evaluated from averages over *typical* blocked configurations: the corresponding Edwards measure is constructed and the predictions compared with the long-time out-of-equilibrium dynamics. In particular, the connection of the fluctuation–dissipation effective temperatures with the entropy of blocked configurations will appear. Finally, in section 4 we show how to obtain some dynamic features, such as the relaxation exponent, aging and density profiles, from a non-linear diffusion model. The approach also allows the analytical investigation of the non-equilibrium stationary states generated by a chemical potential difference and predicts peculiar non-linear transport properties.

2. The Kob–Andersen model

Our starting point is a kinetic lattice-gas model introduced by KA [20]. The system consists of N particles in a cubic lattice of size L^3, with periodic boundary conditions. There can be at most one particle per site. Apart from this hard-core constraint there are no other static interactions among the particles. At each time step a particle and one of its neighbouring sites are chosen at random. The particle moves if the three following conditions are all met:

(i) the neighbouring site is empty;
(ii) the particle has less than ν nearest neighbours;
(iii) the particle will have less than ν nearest neighbours after it has moved.

The rule is symmetric in time, detailed balance is satisfied and all allowed configurations have the same statistical weight in equilibrium. Significant results are obtained when the value of ν is set to 4. With this simple definition one can proceed to study the dynamical behaviour of the model at equilibrium. The kinetic constraints have the physical features associated with the cage effect in high-density liquids. They prevent the particle from moving when it has too many neighbours; the detailed balance condition ensures that equally the particle cannot move if it *would have* too many neighbours after the move. As a consequence, the evolution of the system slows down and becomes sluggish when the particle density ρ increases: when

ρ approaches $\rho_c = 0.881$ the self-diffusion constant D vanishes as a power law

$$D(\rho) \sim (\rho_c - \rho)^{\phi} \tag{1}$$

with an exponent $\phi \simeq 3.1$ [20]. We refer the reader to the original work of KA for a detailed description of the equilibrium dynamics results and their comparison with the predictions of mode-coupling theory. In what follows we shall mainly be concerned with the non-equilibrium dynamics of a version of the KA model in which particle exchange with a reservoir is allowed. The particle reservoir is implemented by allowing creation/destruction of particles in a single layer with the usual Monte Carlo (MC) rule: if a randomly chosen site on the layer is empty, a new particle is added; otherwise the particle is removed with probability $e^{-\beta\mu}$. This sweep is alternated with the ordinary diffusion sweep. In this *canonical* version of the model the number of particles (which plays the role of the energy) is no longer fixed and the external control parameter is the inverse chemical potential $1/\mu$, which plays the role of the temperature.

2.1. Thermodynamics

Before considering the non-equilibrium glassy regime it is important to study the static properties of the KA model. The point is relevant for the question of whether the glass transition is purely dynamical or is a consequence of an equilibrium transition. In the canonical version of the model the Hamiltonian is

$$\mathcal{H} = -\mu \sum_{i=1}^{N} n_i \tag{2}$$

where $n_i = 0, 1$ are the occupation site variables and μ is the chemical potential. The partition function corresponding to the Hamiltonian (2) is

$$\Xi = (1 + e^{\beta\mu})^{L^3}. \tag{3}$$

It would describe correctly the thermodynamics of the system provided irreducibility holds. It is possible to convince oneself that the kinetic rules, which satisfy detailed balance, allow an initially empty lattice to be progressively filled in, leaving only $O(1/L)$ empty sites per unit volume. Indeed, it is always possible to find a path connecting almost any two allowed configurations, if necessary by letting the particles escape one by one by the way they got in. Therefore the Markov process generated by the dynamic evolution rule is irreducible on the configuration space and the static properties of the model are described by (3). In particular the equation of state and the entropy are given respectively by

$$1/\rho = 1 + e^{-\beta\mu} \tag{4}$$

$$s = -\rho \log \rho - (1 - \rho) \log(1 - \rho). \tag{5}$$

(The values of μ and s corresponding to the threshold density ρ_c can be estimated from these equations and are given by $\mu_c \simeq 2.0$, and $s_c \simeq 0.35$.) Since the static properties of the system are regular functions of the density or the chemical potential, the glassy behaviour either is a consequence of a dynamic transition or is a purely kinetic effect.

It is interesting to show irreducibility in a different ensemble in which the particle number is fixed. This is conveniently done by coupling the particle position to an external field such as gravity. In the presence of gravity the system is described by the Hamiltonian

$$\mathcal{H} = mg \sum_{i=1}^{N} h_i n_i \tag{6}$$

where g is the gravity constant, h_i is the height of particle n_i and m is the particle mass. In particular, one can consider a body-centred cubic (BCC) lattice (where every site has eight

nearest neighbours) and the value $\nu = 5$ in the kinetic rule. In this case particles satisfying the kinetic constraints can move according to the Metropolis rule with probability $\min[1, \mathrm{e}^{-\beta g \Delta h}]$, where $\Delta h = \pm 1$ is the vertical displacement in the attempted elementary move. The Markov process generated by the kinetic rules is irreducible on the configuration space provided that the box height is large enough: indeed, it is always possible to find a path connecting any two configurations by letting particles expand in the whole box. Therefore the static properties of the model are, even in this case, those of a non-interacting lattice gas in a gravity field and the glassy behaviour cannot be a consequence of an equilibrium phase transition.

2.2. History dependence and Kauzmann's paradox

The introduction of particle exchange with a reservoir allows the investigation of the non-equilibrium dynamics in the glassy phases of the KA model [23]. This can be done by letting the inverse chemical potential $1/\mu$ decrease or increase smoothly as in cooling or heating experiments. The situation becomes analogous to the *canonical* case in which one controls the temperature, and the energy tries to reach its equilibrium value. In close resemblance to the behaviour of real glasses one obtains curves which exhibit the characteristic annealing-rate dependence of one-time observables. When the relaxation time of the system exceeds the inverse of the annealing rate r, the dynamics become so sluggish that the system is no longer able to keep the pace of the annealing procedure. The faster the compression, the sooner the system falls out of equilibrium [23]. In particular, when one performs a loop in the chemical potential, the density appears to follow a hysteresis cycle (the 'reheating' branch *crossing* the equilibrium curve) whose area decreases as the annealing rate decreases [35]. As is usually done in experiments, once the experimental equation of state is obtained, one can then evaluate the entropy variation of the reservoir by numerical integration, which is given by

$$s(\mu_\mathrm{f}) = s(\mu_\mathrm{i}) - \beta \int_{\mu_\mathrm{i}}^{\mu_\mathrm{f}} \mu \frac{\mathrm{d}\rho}{\mathrm{d}\mu}\, \mathrm{d}\mu. \tag{7}$$

In the absence of irreversibility effects this calorimetric entropy is equal to the thermodynamic one. In figure 1 we see that when the relaxation time exceeds the inverse of the annealing rate the numerical data depart from the equilibrium curve. The point where this first happens defines the laboratory glass transition, $1/\mu_\mathrm{g}(r)$. It is instructive to consider the hypothetical situation in which the annealing rate of the experiment approaches zero. In this limit and in the absence of a dynamic transition, the entropy data would follow the equilibrium curve even below the threshold entropy $s_\mathrm{c} = s(\rho_\mathrm{c}) \simeq 0.35$. One then would feel tempted to extrapolate the value of $1/\mu_\mathrm{g}(r)$ to some non zero Kauzmann 'temperature' $1/\mu_\mathrm{K}$, unless one is able to reach exceedingly low annealing rates (see figure 1). According to this argument, generally known as Kauzmann's paradox, a thermodynamic phase transition at a finite $1/\mu_\mathrm{K}$ would intervene to prevent the entropy from becoming negative. Here there is no clear signature of such a static transition: in this simple case we have access to the complete equilibrium curves, which are perfectly analytical even though they change concavity rather sharply. This provides a simple example of how the distinction between the *ideal* (static or dynamic) and the *laboratory* (i.e. kinetic) glass transition can be very subtle and elusive.

2.3. Structural relaxation

We now turn to the study of the non-equilibrium behaviour of the system after a sudden subcritical quench, which is represented here by a jump in $1/\mu$ from above to below $1/\mu_\mathrm{c}$. In order to allow the system to reach the asymptotic regime more rapidly one performs a 'gentle' quench, i.e. one starts from a configuration with density corresponding to a chemical potential closer to

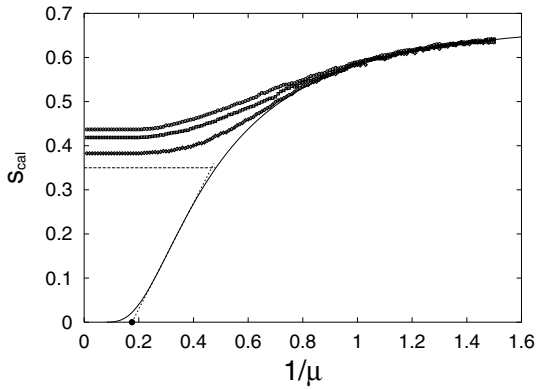

Figure 1. Calorimetric entropy as obtained by thermodynamic integration of compression experiment data for three different annealing rates r. The smooth curve represents the equilibrium entropy equation (5). The laboratory glass transition temperature, $1/\mu_g(r)$, is the departure point of the calorimetric entropy from the equilibrium entropy. The dashed curve shows the threshold value of the entropy corresponding to the dynamic transition, $s_c = s(\rho_c) \simeq 0.35$. The circle located at $1/\mu_K = 0.175$ corresponds to the putative Kauzmann temperature presumably obtained from the extrapolation of $1/\mu_g(r)$ to very slow annealing (dotted curve).

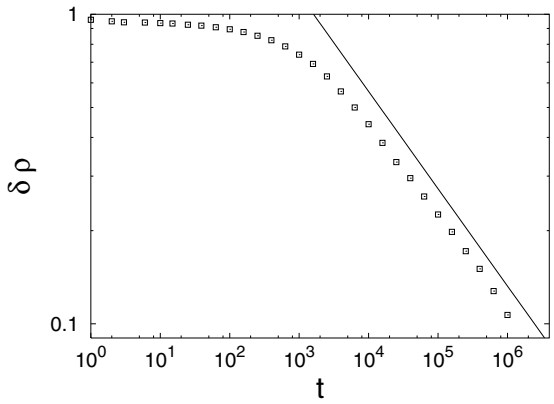

Figure 2. Time relaxation of the excess density $\delta\rho(t) = (\rho_c - \rho(t))/(\rho_c - \rho(0))$, after a subcritical quench to $\mu = 2.2$. The density of the initial configuration is $\rho(0) = 0.75$. The straight line is $\delta\rho \sim t^{-z}$ with $z \simeq 1/\phi$.

μ_c. Figure 2 shows the time relaxation of particle density after a subcritical quench to $\mu = 2.2$, starting from a random configuration with density $\rho(0) = 0.75$. We see that the system is not able to equilibrate on the accessible timescales but instead approaches the threshold density like a power law in time:

$$\rho_c - \rho(t) \sim t^{-z} \tag{8}$$

where t is the time elapsed after the quench and where the exponent $z \simeq 1/\phi$ (with ϕ defined by (1)). The lack of equilibration is essentially due to a *kinetic bottleneck*: at high packing density the number of paths leading to the equilibrium configurations is much smaller than that leading elsewhere. Therefore, even if the dynamics is in principle always able to reach equilibrium, configurations with $\rho \geqslant \rho_c$ are not effectively accessible. This dynamic behaviour is qualitatively similar to that of mean-field glass models [39]. The roles played by the inverse chemical potential and the inverse density are analogous to those played by temperature and energy in the mean-field case, respectively. When quenched below T_c, mean-field spin-glass models never equilibrate. Their energy relaxes to a dynamic threshold value $E_{th}(T)$ which is

higher than the equilibrium one, and can be characterized as the value below which the phase space breaks into disconnected components [39]. In our case, the moves allowed by the kinetic constraints keep the configuration space of the system effectively connected only for $\rho < \rho_c$. Of course, it is hard to establish from numerical simulations the existence and the nature of such a dynamic transition in the KA model, and one is led to wonder about a possible system-size dependence of these results. For a detailed discussion of finite-size effects in the KA model, see [20]. We just mention here that a comparison with the backbone percolation problem shows that the dependence of the critical threshold on the linear system size L cannot be faster than [20]

$$1 - \rho_c(L) \sim 1/\log(\log L). \tag{9}$$

Therefore even if $\lim_{L\to\infty} \rho_c(L) = 1$, (i.e. if there is no dynamic transition), the length-scale for which $\rho_c \approx 1$ would be observable is not experimentally accessible.

It has been suggested that the power-law behaviour of the diffusion constant as a function of the density is reminiscent of critical phenomena (and it should be related to the existence of a diverging length) [36]. If this is the case, one would expect on the basis of universality arguments that the exponent ϕ should not depend upon the details of the dynamics, while the threshold density should show such a dependence. This conjecture has been verified for systems on a face-centred cubic (FCC) lattice [36] and on a BCC lattice [49].

2.4. Aging and chaoticity

The power-law behaviour of the density relaxation implies that, after a subcritical quench, time-translation invariance is broken. In fact, consider the two-time mean-squared displacement of particles defined as

$$B(t, t_w) = \frac{1}{3N} \sum_{a=1}^{3} \sum_{k=1}^{N} \langle [r_k^a(t + t_w) - r_k^a(t_w)]^2 \rangle \tag{10}$$

where $r_k^a(t)$ and $r_k^a(t_w)$ are the coordinates ($a = 1, 2, 3$) of the same particles k at times t and t_w respectively. The average must be defined with some care, since particles may leave or enter the system. We define it by averaging only over the particles which are present at both times. At sufficiently large time separations the mean squared displacement would be given by

$$B(t, t_w) = \int_{t_w}^{t+t_w} d\tau \; D(\rho) \tag{11}$$

where $D(\rho)$ is the diffusion coefficient given by equation (1). Therefore, if $\rho_c - \rho(t) \sim t^{-1/\phi}$ the diffusion coefficient in the glassy phase vanishes as

$$D(t) \sim t^{-1} \tag{12}$$

from which a logarithmic *simple* aging follows:

$$B(t, t_w) \sim \log\left(1 + \frac{t}{t_w}\right) \tag{13}$$

in good agreement with the numerical results [33]. This relation implies the weak-ergodicity breaking property [39]:

$$\lim_{t_w\to\infty} \lim_{t\to\infty} B(t, t_w) = \infty. \tag{14}$$

This means that, no matter how large t_w is, the trajectory of the system wanders away from any region of configuration space at sufficiently long time t. Further insight into the aging dynamics is obtained by studying its 'chaoticity' property [39]. After aging for a time t_w, one duplicates the system and subsequently evolves the two copies (clones) with different

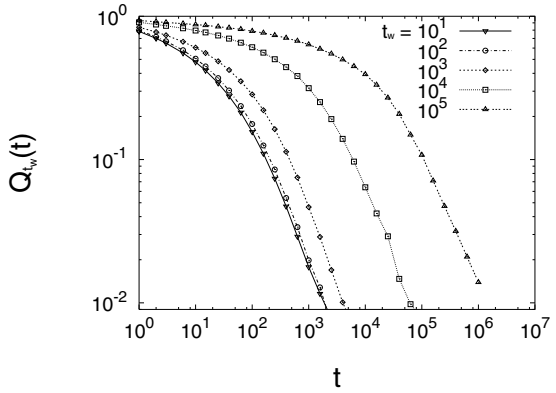

Figure 3. Mean overlap $Q_{t_w}(t)$ between two clones after a subcritical quench in the glassy phase ($\mu = 2.2$): the two clones are separated at time t_w and evolve subsequently with different realizations of noise. $Q_{t_w}(t)$ always decreases to zero (the slower the larger t_w), showing that the trajectories of the clones in the configuration space always tend to diverge.

realizations of the thermal noise (corresponding to different sequences of random numbers in the updating procedure of MC dynamics). The question is then whether or not the trajectories diverge at an arbitrary large time. This is measured by the overlap function $Q_{t_w}(t)$ defined here as

$$Q_{t_w}(t) = \left\langle \frac{\sum_i n_i^1(t) n_i^2(t) - N\rho^1(t)\rho^2(t)}{\sum_i n_i^1(t_w) n_i^2(t_w) - N\rho^1(t_w)\rho^2(t_w)} \right\rangle \tag{15}$$

where the superscript $a = 1, 2$ denotes the two clones and the brackets denote the average over different realizations of the randomness. Figure 3 reports the results for $Q_{t_w}(t)$ for several values of t_w, showing that

$$\lim_{t_w \to \infty} \lim_{t \to \infty} Q_{t_w}(t) = 0. \tag{16}$$

In other words, no matter how large t_w is, the two trajectories always become as far as possible from each other in the configuration space. Thus, while the breakdown of time-translation invariance seems to rule out the possibility of a thermodynamic description, the last two features seem to suggest the existence of a form of ergodicity associated with the aging behaviour.

2.5. Fluctuation–dissipation effective temperature

A subtle consequence of mean-field aging dynamics is a peculiar pattern of violation of the fluctuation–dissipation theorem (FDT) [39]. It allows the definition of a timescale-dependent effective temperature $T_{\rm dyn}$ [40], which is the first signature of a hidden form of ergodicity underlying the glassy phase [41–43].

In our case, the effective temperature can be defined by comparing the two-time mean-square displacement $B(t, t_w)$ and the mobility $\chi(t, t_w)$ between two widely separated times t and t_w [34]. The mobility is obtained by applying a random stirring force to the particles at time t_w after quenching the system into the glassy phase:

$$\mathcal{H}_\epsilon = \epsilon \sum_{a=1}^{3} \sum_{k=1}^{N} f_k^a \, r_k^a \tag{17}$$

where $f_k^a = \pm 1$ independently for each coordinate a and particle k at position r_k^a. The linear response regime is probed for small enough values of the perturbation strength ϵ. In the

presence of the perturbation, a local elementary move which satisfies the kinetic constraints is accepted with probability $\min[1, \mathrm{e}^{-\beta\epsilon\, \boldsymbol{f}\cdot\delta\boldsymbol{r}}]$, where $\boldsymbol{f}\cdot\delta\boldsymbol{r} = \pm 1$ is the displacement in the attempted move. (We write the temperature $T = 1/\beta$ explicitly, though it is always understood that $T = 1$.) The integrated response function is given by

$$\kappa(t, t_{\mathrm{w}}) = \frac{1}{3N}\sum_{a=1}^{3}\sum_{k=1}^{N}\left\langle f_k^a\, \Delta r_k^a(t + t_{\mathrm{w}})\right\rangle \tag{18}$$

where $\Delta r_k^a(t + t_{\mathrm{w}})$ is the mean displacement at time $t + t_{\mathrm{w}}$ from the configuration at time t_{w} in the presence of the perturbation. This quantity can be conveniently measured by considering the difference between the displacements at time $t + t_{\mathrm{w}}$ in the presence of a perturbation and in its absence (while evolving the two systems with the same sequence of random numbers). The integrated version of the generalized FDT [39] yields a relation between $\kappa(t, t_{\mathrm{w}})$ and $B(t, t_{\mathrm{w}})$:

$$\kappa(t, t_{\mathrm{w}}) = \frac{\epsilon}{2T}\int_0^{B(t,t_{\mathrm{w}})} X(B)\,\mathrm{d}B. \tag{19}$$

The fluctuation–dissipation ratio $X(B)$ is a measure of the violation of FDT. If FDT holds, $X(B) = 1$ and

$$\kappa(t, t_{\mathrm{w}}) = \frac{\epsilon}{2T}\, B(t, t_{\mathrm{w}}) \tag{20}$$

so $\kappa(t, t_{\mathrm{w}})$ is a linear function of $B(t, t_{\mathrm{w}})$ with slope $\epsilon/2T$. A deviation from this straight line therefore indicates a failure of FDT. The way in which FDT breaks down plays a key role since it can show the presence of an effective temperature for the slow modes associated with the structural rearrangement. One observes two asymptotic regimes similar to those found in the out-of-equilibrium dynamics of mean-field structural glasses: a short-time quasi-equilibrium regime where FDT holds, and, at larger separation times, a regime in which a violation FDT with a constant factor $X \simeq 0.79$ occurs. These results appear clearly in the parametric plot of $\kappa(t, t_{\mathrm{w}})$ versus $B(t, t_{\mathrm{w}})$ where the curve approaches the characteristic broken curve (see figure 4). A similar violation pattern has been observed in the KA model on an FCC lattice [36], and in the presence of gravity on a BCC lattice [48] (see figure 5). It is also interesting to consider the behaviour of a binary mixture of particles with two different kinetic constraints. In this case one observes a purely dynamic gravity-driven phase separation where more constrained particles segregate towards the top of the mixture [37]. Two different fluctuation–dissipation temperatures appear in this regime, the smaller one being associated with the less constrained particles.

3. Edwards' measure

Given the non-holonomic nature of kinetic constraints and the trivial Hamiltonian of the model, one might wonder whether a statistical mechanics approach based on the calculation of some restricted partition function would ever be able to predict some features of the glassy phase. For example, at a given long time, when the system has reached a high packing density $\rho(t)$, one may wish to measure the structure factor $g(r, \rho)$, or the value of the effective temperature $T_{\mathrm{dyn}}(\rho)$.

Some years ago, in a granular matter context, Edwards proposed that one could reproduce the observables measured in the stationary state of a tapping dynamic experiment by calculating the value they take in the usual equilibrium distribution at the corresponding volume, energy etc *but restricting the sum to the blocked configurations* defined as those in which every particle is unable to move [44]. This Edwards measure leads immediately to the definition of an entropy S_{Edw} as the logarithm of the number of blocked configurations of given volume, energy etc, and its corresponding density $s_{\mathrm{Edw}} \equiv S_{\mathrm{Edw}}/N$. Associated with this entropy are state variables

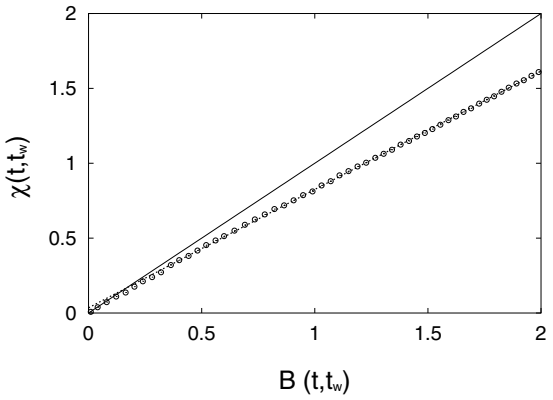

Figure 4. Measuring the non-equilibrium fluctuation–dissipation relation in a zero-gravity compaction experiment. Parametric plot of the mobility $\chi(t, t_w) = 2\kappa(t, t_w)/\epsilon$ versus the mean-square displacement $B(t, t_w)$. The system is prepared in a random initial configuration with density $\rho = 0.75$ and then a subcritical quench into the glassy phase at chemical potential $\mu = 2.2$ ($\mu_c \simeq 2.0$) is performed. The perturbation ($\epsilon = 0.1$) is applied at waiting time $t_w = 10^5$. The full line corresponds to the equilibrium FDT (slope $T = 1$). In the aging phase the nature of the FDT violation allows one to define an effective temperature T_{dyn} (the slope of the dashed curve is $T_{dyn}^{-1} \simeq 0.79$).

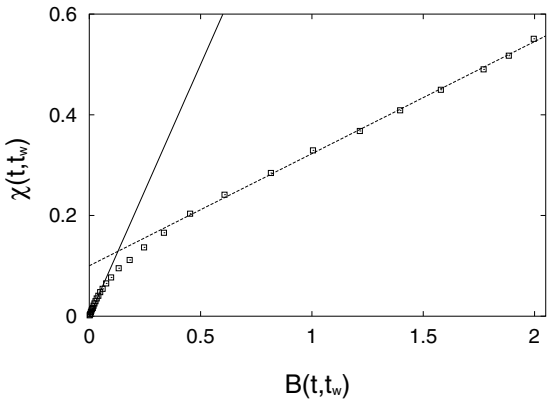

Figure 5. Measuring the non-equilibrium fluctuation–dissipation relation in a compaction experiment under gravity. Parametric plot of the mean-square displacement $B(t, t_w)$ versus the conjugate response function $\chi(t, t_w)$. The system is prepared in a random loose-packed configuration, $\rho_{rlp} \simeq 0.707$. The gravity temperature ratio is $\beta g \simeq 1.61$. The waiting time after which the random stirring force is turned on is $t_w = 2^{14}$. The slope of the full line corresponds to the equilibrium fluctuation–dissipation temperature ($T = 1$). The slope of the dashed line is $T_{dyn}^{-1} \simeq 0.22$.

such as 'compactivity' $X_{Edw}^{-1} = (\partial/\partial V)S_{Edw}(V)$ and 'temperature' $T_{Edw}^{-1} = (\partial/\partial E)S_{Edw}(E)$. Mean-field glass theory predicts that the temperature T_{Edw}, despite its different origin, matches exactly the T_{dyn} obtained from the fluctuation–dissipation relation during the aging dynamics at almost zero temperature (see [41–43] and references therein).

The nature of the KA model makes it a good candidate for testing Edwards' hypothesis in finite dimensions [45]. In this context, we consider a flat measure over blocked configurations *that have the density $\rho(t)$ of the dynamic situation we wish to reproduce*. This means that we

have given up trying to predict the dynamic evolution of the density by methods other than the dynamics itself. We therefore compute say the structure factor in *all the possible* blocked configurations of density $\rho(t)$, and calculate the average. Thus, the only input from dynamics is $\rho(t)$, apart from which the calculation is based on a statistical ensemble. That configurations with low mobility should be relevant in a jammed situation is rather evident; the strong hypothesis here is that the configurations reached dynamically are *the typical ones* of given density.

3.1. The auxiliary model

To construct the Edwards measure explicitly one has to devise a method for counting and calculating averages over blocked configurations [45]. The expectation values thus obtained can then be compared with equilibrium values and with the results of the aging dynamics. This can be done by means of an auxiliary model in which particles have energy equal to unity if the dynamic rule of the KA model allows them to move, and to zero otherwise. The auxiliary Hamiltonian of the KA model is therefore highly complicated, involving next-nearest-neighbour interactions (and hence its thermodynamics is non-trivial). We can now introduce an auxiliary temperature $1/\beta_{\rm aux}$ associated with the auxiliary energy $E_{\rm aux}$ (equal to the number of particles that are able to move) and perform simulated annealing at fixed number of particles: at low $\beta_{\rm aux}$ all configurations are sampled uniformly, while as $\beta_{\rm aux}$ grows sampling is restricted to configurations with a vanishing fraction of moving particles. Efficient sampling is achieved by means of *non-local* moves (accepted with a standard Metropolis probability $\min\{1, \exp(-\beta_{\rm aux}\Delta E_{\rm aux})\}$). In this way, one obtains the equilibrium energy density of the auxiliary model, $e_{\rm aux}(\beta_{\rm aux}, \rho)$, and its entropy density, $s_{\rm aux}(\beta_{\rm aux}, \rho)$, by thermodynamic integration:

$$s_{\rm aux}(\beta_{\rm aux}, \rho) = s_{\rm eq}(\rho) + \beta_{\rm aux}\, e_{\rm aux}(\beta_{\rm aux}, \rho) - \int_0^{\beta_{\rm aux}} e_{\rm aux}(\beta, \rho)\, {\rm d}\beta. \tag{21}$$

We set $s_{\rm aux}(0, \rho) = s_{\rm eq}(\rho)$, since the limit $\beta_{\rm aux} \to 0$ corresponds to the equilibrium measure. The energy of the auxiliary model was computed in the range $\rho \in [0.65, 0.95]$ with a step in density $\Delta\rho = 0.005$ and for $\beta_{\rm aux} \in [0, 20]$ with a step $\Delta\beta_{\rm aux} = 0.1$. In figure 6 we show a subset of data concerning the energy and entropy density as obtained by thermodynamic integration. It is clear from figure 6 that the limit of our interest corresponding to the Edwards measure, $\beta_{\rm aux} \to \infty$, is already approached for $\beta_{\rm aux} \simeq 5$. To evaluate the observables within the Edwards' measure we now consider the limit $\beta_{\rm aux} \to \infty$ of the observables computed in the auxiliary model. The Edwards entropy is then obtained as

$$s_{\rm Edw}(\rho) \equiv \lim_{\beta_{\rm aux}\to\infty} s(\beta_{\rm aux}, \rho) = s_{\rm eq}(\rho) - \int_0^{\infty} e_{\rm aux}(\beta, \rho)\, {\rm d}\beta \tag{22}$$

since

$$\lim_{\beta_{\rm aux}\to\infty} \beta_{\rm aux}\, e_{\rm aux}(\beta_{\rm aux}, \rho) = 0. \tag{23}$$

In figure 7 we plot the Edwards and the equilibrium entropy as a function of the particle density. It is clear that the most typical blocked configurations ($\rho \simeq 0.75$) are irrelevant as far as the compaction dynamics is concerned. Since the relation between chemical potential, temperature and entropy density at equilibrium is given by (4) and (5), the natural definition for Edwards' temperature is

$$T_{\rm Edw}^{-1} = -\frac{1}{\mu}\frac{{\rm d}s_{\rm Edw}}{{\rm d}\rho}. \tag{24}$$

At fixed density it can be rewritten, by using $-\beta\mu = {\rm d}s_{\rm eq}/{\rm d}\rho$, as

$$T_{\rm Edw}(\rho)\frac{{\rm d}s_{\rm Edw}}{{\rm d}\rho} = T(\rho)\frac{{\rm d}s_{\rm eq}}{{\rm d}\rho}. \tag{25}$$

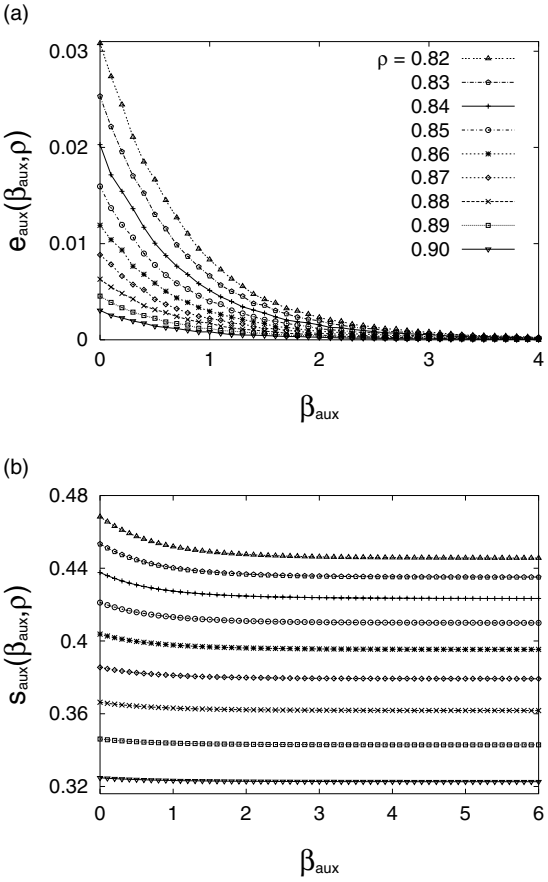

Figure 6. Thermodynamic properties of the auxiliary model. (*a*) Energy density $e_{\rm aux}$ versus inverse temperature $\beta_{\rm aux}$ at different particle densities ρ. (*b*) Entropy density $s_{\rm aux}$ as obtained from thermodynamic integration of the energy data.

The agreement between $T_{\rm dyn}(t_{\rm w})$ obtained from the fluctuation–dissipation relation, and $T_{\rm Edw}(\rho)$ obtained from the blocked configurations for the density $\rho = \rho(t_{\rm w})$ at which the dynamical measurement were made, is excellent. Similarly, the Edwards measure structure function at a given density, $g_{\rm Edw}(r, \rho)$, is obtained as

$$g_{\rm Edw}(r, \rho) = \lim_{\beta_{\rm aux}\to\infty} g_{\rm aux}(r, \rho, \beta_{\rm aux}). \tag{26}$$

In figure 8 we plot the dynamical $g_{\rm dyn}(r, \rho, t)$, the equilibrium $g_{\rm eq}(r, \rho) = \rho^2$ and the Edwards $g_{\rm Edw}(r, \rho)$ structure factors, for the same density $\rho \simeq 0.87$. While $g_{\rm eq}(r, \rho)$ is flat, the system has developed short-range correlations in the slow-annealing procedure, which seem to be reproduced rather well by $g_{\rm Edw}(r, \rho)$.

Is it possible to obtain the Edwards entropy from a structural characteristic (in an experiment or in a simulation)? We suggest here a method which is based on the possibility of expressing the excess entropy of a simple fluid in terms of multi-particle correlations [46, 47]. In the 'two-body' approximation it reads

$$s^{(2)}(\rho) = -2\pi\rho \int_0^\infty [g(r, \rho) \ln g(r, \rho) - g(r, \rho) + 1]\, r^2\, {\rm d}r. \tag{27}$$

If the Edwards hypothesis holds true, a straightforward generalization of the previous relation would give a way to estimate the entropy of blocked configurations from measurements of the structure function in aging, tapping or shearing experiments.

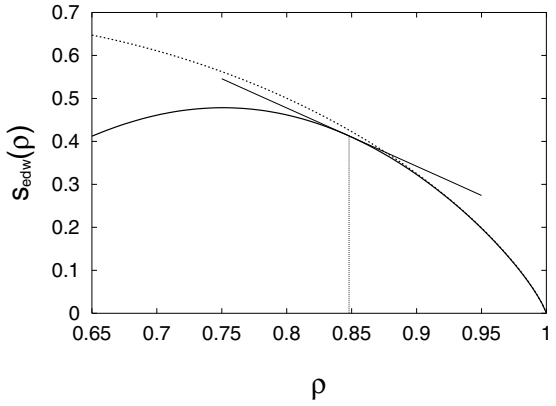

Figure 7. Edwards entropy density versus particle density (full curve) as obtained from the zero-temperature entropy of the auxiliary model. For comparison we also show the equilibrium entropy (dashed curve). At high enough density the curves are indistinguishable, and join exactly only at $\rho = 1$. The slope of the tangent to $s_{\mathrm{Edw}}(\rho)$ for a generic ρ allows us to extract $T_{\mathrm{Edw}}(\rho)$ from the relation $T_{\mathrm{Edw}}(\rho)\mathrm{d}s_{\mathrm{Edw}}/\mathrm{d}\rho = T(\rho)\mathrm{d}s_{\mathrm{eq}}/\mathrm{d}\rho$. At $\rho(t_{\mathrm{w}}) = 0.848$ one obtains the effective temperature measured during the aging dynamic experiment of figure 4.

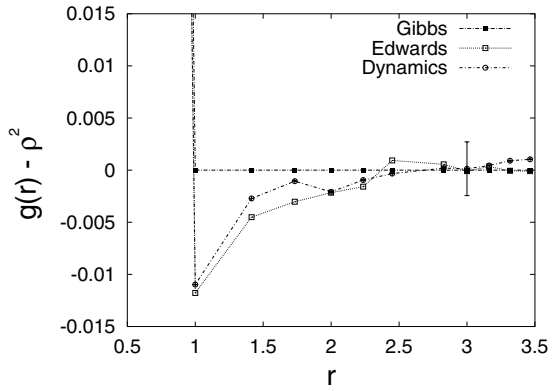

Figure 8. Structure functions $g(r) - \rho^2$ at density $\rho \simeq 0.87$ computed with the equilibrium, Edwards and dynamic measures. The three sets of data originate from independent MC simulations. The dynamic structure function (circles) is obtained after a very slow compression by raising the chemical potential from $\mu = 1$ to 3 with a step of $\Delta\mu = 0.01$ every 10^4 MC sweeps; it is measured in the centre of the box where the homogeneity of the system was checked. The Edwards structure function (open squares) is obtained from the auxiliary model at $\beta_{\mathrm{aux}} = 10$. Although the equilibrium value of $g(r) - \rho^2$ is exactly zero, we also obtain it by a MC simulation (full squares) in order to show that the difference in the short-distance behaviour is not an artifact of the numerical simulation. The size of the typical error bar on dynamic data is shown at $r = 3$.

4. Mean-field dynamics

In this section we show how some of the results reported in section 2 can be understood in terms of a non-linear diffusion model. We consider the sample as a slab, whose free surfaces at $z = \pm L$ are in contact with the reservoir and therefore rapidly reach a density equal to the equilibrium one. We then assume that within the sample, the particle density $\rho(z, t)$ satisfies

the following non-linear diffusion equation:

$$\frac{\partial \rho}{\partial t} = \frac{\partial}{\partial z}\left[D_\phi(\rho) \frac{\partial \rho}{\partial z} \right] \tag{28}$$

with the boundary conditions $\rho(\pm L) = \rho_R \leqslant \rho_c$, and where $\rho(z,t) \leqslant \rho_R$ for $|z| < L$ and all t. The diffusion coefficient is given by $D_\phi(\rho) = D_0(1+\phi)(\rho_c - \rho)^\phi$, where $\phi \simeq 3.1$ as found by KA [20]. Changing the variable to $y(z,t) = \rho_c - \rho(z,t)$, we obtain the equation

$$\frac{\partial y}{\partial t} = D_0(\phi+1)\left[\phi y^{\phi-1} \left(\frac{\partial y}{\partial z} \right)^2 + y^\phi \frac{\partial^2 y}{\partial z^2} \right]. \tag{29}$$

In the low-density phase, $\rho_R \ll \rho_c$, the non-linearities of equation (29) are expected to be irrelevant and the relaxation towards the equilibrium distribution should be exponential. Linearizing equation (29) around the equilibrium state, $\rho_{eq}(z,t) = \rho_R$, one finds that the characteristic relaxation time is

$$\tau(\rho_R) \sim (\rho_c - \rho_R)^{-\phi} \tag{30}$$

which as expected diverges as $\rho_R \to \rho_c$ with an exponent $-\phi$. In the high-density phase, $\rho_R = \rho_c$, the density of the edge layers closely approaches the critical threshold, and hence slow relaxation and aging are expected. If one now looks for solutions of the form $y(z,t) = f(z)g(t)$, one obtains a power-law relaxation of the density with an exponent $1/\phi$, $g(t) \sim t^{-1/\phi}$ as found in simulations (see figure 2), and a differential equation for the density profile $f(z)$:

$$f(z) = \frac{\partial}{\partial z}[f^\phi(z) f'(z)] \tag{31}$$

with the boundary conditions

$$f(\pm L) = 0. \tag{32}$$

The asymptotic scale-invariant solution of the density profile is discussed in [33]. Here, we present in figure 9 the time evolution of the density profile obtained from the numerical integration of equation (28). The comparison with the profiles obtained in MC simulations shows that the non-linear diffusion model reproduces the overall spatial distribution of the particle density rather well. The deviations observed near the edges are a discretization/finite-size effect, as the density of a *single* two-dimensional layer can be higher than that allowed by the kinetic constraint. They therefore occur at high density and are expected to disappear in the thermodynamic limit. As previously discussed the effect of a varying diffusion constant implies that the mean-square displacement $B(t, t_w)$ has a logarithmic *simple* aging behaviour. This is compatible with the 'triangle relation':

$$B(t,t') = B(t,s) + B(s,t') \qquad \text{for} \quad t' < s < t \tag{33}$$

which stems from the statistical independence of particle displacements over non-overlapping time intervals. Note that the factorization property of the solution, $y(z,t) = f(z)g(t)$, tells us that the specific form of temporal correlations does not depend on the presence of a non-homogeneous density profile.

It is a simple matter to generalize the non-linear diffusion model to the case when gravity is present [49]. In this case two temporal scales appear: one associated with the diffusion time $\tau_1 \propto L^2$, and the other one with the drift time $\tau_2 \propto L/\gamma$, where $\gamma = mg/k_B T$ is the inverse gravitational length. The asymptotic scaling analysis of the model shows that gravity changes the dynamic relaxation exponent and the nature of aging behaviour. One finds that in

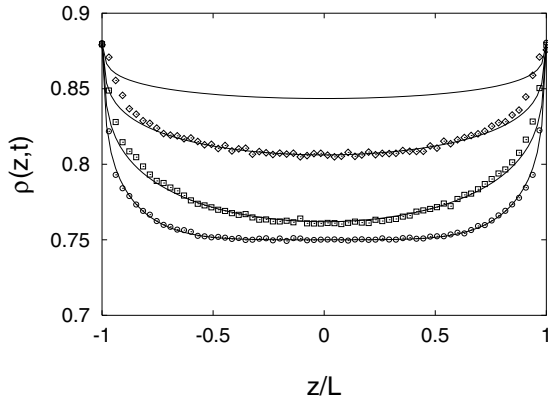

Figure 9. Density profile $\rho(z,t)$ versus z/L at MC time $t = 10^3$ (circle), $t = 10^4$ (square) and $t = 10^5$ (diamond), after a quench at $\rho = 0.88$, starting from a random initial configuration with density $\rho = 0.75$, for system size $L = 64$ with transverse surface 32^2. The continuous curves are the curves obtained from the numerical integration of the diffusion equation; the upper curve would correspond to a profile at the MC time $t = 10^6$. We have chosen the KA value of $\phi = 3.1$ and $\rho_c = 0.88$.

the bottom layer of the box, the relaxation time diverges with an exponent $\phi - 2$, while the density relaxation still follows a power-law

$$\rho_c - \rho(z,t) \sim \left(\frac{z}{\phi\gamma\ t}\right)^{1/(\phi-1)} . \tag{34}$$

In particular, to leading order in t and t_w, the mean-square displacement goes like

$$B(t,t_w) \sim t_w^{1-\mu} - t^{1-\mu}. \tag{35}$$

The exponent $\mu = \phi/(\phi-1)$ corresponds to a super-aging regime ($\mu > 1$) when $\phi > 1$. A similar scaling behaviour is observed in the simulation of the gravity-driven KA model [48].

4.1. Non-equilibrium stationary states

One might wonder what the effects of blocked configurations are when the system is driven into a non-equilibrium stationary state by non-relaxational forces. A rather natural situation that can be analytically investigated in the present context is that in which the system is simultaneously in contact with two particle reservoirs and a stationary current flows through the system. Consider then the system boundaries, located at $z = \pm L$, in diffusive contact with two reservoirs at different chemical potential $\mu_\pm$. The global effect of the reservoirs is to keep the boundary densities at two different values $\rho_\pm$

$$\rho(\pm L,t) = \rho_\pm \qquad \forall t \geqslant 0. \tag{36}$$

When $\rho_+ = \rho_- < \rho_c$, the characteristic relaxation time is finite and the system attains an equilibrium state characterized by a flat profile. When $\rho_+ \neq \rho_-$ and ρ_+, $\rho_- < \rho_c$, the relaxation time is still finite for any finite L, and the steady-state density profile is

$$\rho_c - \rho(z) = (L\,a_+ - z\,a_-)^{\frac{1}{1+\phi}} \tag{37}$$

where the constants $a_\pm$ are determined by the boundary condition (36),

$$a_\pm = \frac{1}{2L}\big[\,(\rho_c - \rho_-)^{1+\phi} \pm (\rho_c - \rho_+)^{1+\phi}\,\big]. \tag{38}$$

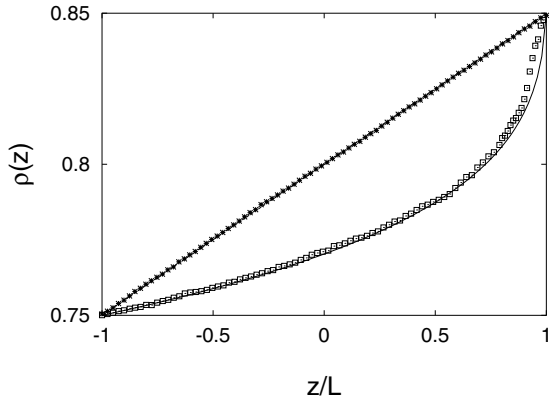

Figure 10. Density profile in a boundary-driven lattice glass coupled to two particle reservoirs at density $\rho_+ = \rho(L) = 0.85$ and $\rho_- = \rho(-L) = 0.75$ (squares), with $L = 160$ and transverse surface 20^2. The continuous smooth curve represents the analytic profile predicted by the diffusion equation, equation (37) (with the KA value of $\phi = 3.1$ and $\rho_c = 0.88$). Also shown, for comparison, are the linear profile corresponding to a normal diffusion coefficient (dashed curve), and the numerical simulation data obtained by removing the kinetic constraint (stars).

In figure 10 the density profile obtained in an MC simulation is compared with that predicted by the anomalous diffusion equation using the value of ρ_c and ϕ found in [20]. The agreement between the two is excellent. The small discrepancy observable near the higher-density edge is a finite-size effect similar to that encountered before, and therefore is expected to disappear as the thermodynamic limit $L \to \infty$ is approached. In figure 10 we also show for comparison the numerical density profile of the usual boundary-driven three-dimensional lattice gas (which is simply obtained by removing the kinetic constraint), and that predicted by the normal diffusion equation. These results suggest that the non-linear nature of the density profile close to the threshold is essentially determined by the presence of blocked configurations induced by the kinetic constraint.

The peculiar non-linear nature of the density profile has far-reaching consequences for the transport properties of the model near the threshold. The particle current can be calculated as $J = D(\rho)\partial_z\rho$, and is therefore given by

$$J(\rho_+, \rho_-) = \frac{D_0}{2L}\big[\,(\rho_c - \rho_-)^{1+\phi} - (\rho_c - \rho_+)^{1+\phi}\,\big]. \tag{39}$$

This expression has two interesting features: it is non-linear and does not depend only on the single variable $\Delta\rho = \rho_+ - \rho_-$. In the limit $\rho_\pm \ll \rho_c$ the density profile is linear, and one correctly recovers Fick's law $J \sim \Delta\rho$, in agreement with linear-response theory. At high enough density, however, this is not the case and more interesting transport phenomena emerge. In the non-linear regime one can show that equation (39) exhibits phenomena such as rectification, negative resistance and hysteresis depending on the way the drive acts on the boundary. An example is shown in figure 11 (for more details, see [51]).

5. Conclusions

In summary, when endowed with a mechanism of particle exchange with a reservoir, the KA model qualitatively reproduces the corpus of mean-field glassy phenomenology, which is the present paradigm of our understanding of the structural glass transition problem. The model exhibits history dependence, hysteresis, power-law approach to the asymptotic state, physical

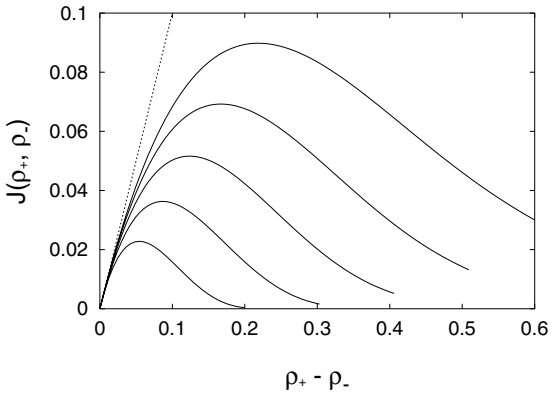

Figure 11. Negative resistance. The particle current $J(\rho_+, \rho_-)$ is plotted versus the driving force $\rho_+ - \rho_-$ for different values of the ratio $\delta = \rho_-/\rho_+ = 0.4, 0.5, 0.6, 0.7, 0.8$ (from top to bottom). Increasing the drive above a threshold value leads to a decreasing particle current. The dotted curve represents Fick's law, which is recovered in the limit of small density gradient.

aging, chaoticity, fluctuation–dissipation effective temperature and, as recently shown, dynamic heterogeneities [50]. A phenomenological non-linear diffusion equation allows one to derive analytically many of the results observed in numerical simulations. It also predicts interesting transport phenomena in the non-equilibrium stationary regime, which could be tested in more realistic models. In some respects these features might appear rather surprising since

(i) the model is non-mean-field and does not contain any quenched disorder or frustration in its Hamiltonian,
(ii) the slowing down of the dynamics does not seem to be related to an underlying thermodynamic transition,
(iii) blocked configurations do not have an *a priori* simple interpretation in terms of local minima of some complex free-energy landscape and
(iv) the phase-space organization of blocked configurations is different from that found in mean-field spin-glasses [50].

Several possible scenarios can be envisaged. We only mention that, if we exclude the existence of a dynamic phase transition (on the basis of a nucleation argument) and a static transition (on the grounds of irreducibility), one is led to accept that the glassy behaviour observed in this model is a merely kinetic effect. This would mean that in the asymptotic limit the system is described by the Gibbs measure (in this case trivial), while in a preasymptotic limit (that observed in simulations) it would be described, due to a bizarre finite-time, finite-size conspiracy, by the glassy mean-field scenario and the Edwards measure.

In spite of its simplicity the KA model still retains much of the enigmatic character of the glass transition.

Acknowledgments

It is a pleasure to thank J J Arenzon, A Barrat, J Kurchan, Y Levin, V Loreto and L Peliti for their contribution to this work, and F Ritort and P Sollich for their comments on the manuscript.

References

[1] Feynman R P 1972 *Statistical Mechanics* (Reading, MA: Addison-Wesley) p 1
[2] Ma S K 1985 *Statistical Mechanics* (Singapore: World Scientific) p 2
[3] Wannier G H 1987 *Statistical Physics* (New York: Dover) p 219
[4] Reiner M 1969 *Phys. Today* **621** 16
Reiner M 1975 *Selected Papers on Rheology* (Amsterdam: Elsevier)

[5] Truesdell C 1980 *Rheology 8th Int. Congress (Naples, 1980)* ed G Astarita, G Marrucci and L Nicolais (New York: Plenum)
[6] Struik L C E 1978 *Physical Aging in Amorphous Polymers and Other Materials* (Amsterdam: Elsevier)
[7] Young A P (ed) 1997 *Spin-Glasses and Random Fields* (Singapore: World Scientific)
[8] Leutheusser E 1984 *Phys. Rev.* A **29** 2765
[9] Bengtzelius U, Götze W and Sjölander A 1984 *J. Phys. C: Solid State Phys.* **17** 5915
[10] Kirkpatrick T R 1985 *Phys. Rev.* A **31** 939
[11] Das S P, Mazenko G F, Ramaswamy S and Toner J 1985 *Phys. Rev. Lett.* **54** 118
[12] Siggia E 1985 *Phys. Rev.* A **32** 3135
[13] Das S P, Mazenko G F, Ramaswamy S and Toner J 1985 *Phys. Rev.* A **32** 3139
[14] Kirkpatrick T R and Wolynes P 1987 *Phys. Rev.* A **35** 3072
[15] Kirkpatrick T R and Thirumalai D 1987 *Phys. Rev.* B **36** 5388
[16] Fredrickson G H and Andersen H C 1984 *Phys. Rev. Lett.* **53** 1244
Fredrickson G H and Andersen H C 1985 *J. Chem. Phys.* **83** 5822
[17] Fredrickson G H and Brawer S A 1986 *J. Chem. Phys.* **84** 3351
[18] Butler S and Harrowel P 1991 *J. Chem. Phys.* **95** 4454
[19] Jäckle J and Eisinger S 1991 *Z. Phys.* B **84** 115
[20] Kob W and Andersen H C 1993 *Phys. Rev.* E **48** 4364
[21] Follana E and Ritort F 1996 *Phys. Rev.* B **54** 930
[22] Graham I S, Piché L and Grant M 1997 *Phys. Rev.* E **35** 2132
[23] Kurchan J, Peliti L and Sellitto M 1997 *Europhys. Lett.* **39** 365
[24] Sollich P and Evans M R 1999 *Phys. Rev. Lett.* **83** 3238
[25] Pitts S J, Young T and Andersen H C 2000 *J. Chem. Phys.* **113** 8671
[26] Crisanti A, Ritort F, Rocco A and Sellitto M 2000 *J. Chem. Phys.* **113** 10 615
Crisanti A, Ritort F, Rocco A and Sellitto M 2002 *J. Phys.: Condens. Matter* in this volume
[27] Garrahan J P and Newman M E J 2000 *Phys. Rev.* E **62** 7670
[28] Fierro A, de Candia A and Coniglio A 2000 *Phys. Rev.* E **62** 7715
[29] Davison L, Sherrington D, Garrahan J P and Buhot A 2001 *J. Phys. A: Math. Gen.* **34** 5147
[30] Kawasaki K and Kim B 2001 *Phys. Rev. Lett.* **86** 3582
[31] Onsager L 1949 *Ann. NY Acad. Sci.* **51** 627
[32] Frenkel D 1999 *Physica* A **263** 26
[33] Peliti L and Sellitto M 1998 *J. Physique* **8** Pr6 49–56
[34] Sellitto M 1998 *Eur. Phys. J.* B **4** 135
[35] Sellitto M 2000 *J. Phys.: Condens. Matter* **12** 6477
[36] Imparato A and Peliti L 2000 *Phys. Lett.* A **269** 154
[37] Sellitto M and Arenzon J J 2000 *Phys. Rev.* E **62** 7793
[38] Mézard M, Parisi G and Virasoro M A 1987 *Spin-Glass Theory and Beyond* (Singapore: World Scientific)
[39] Bouchaud J-P, Cugliandolo L F, Kurchan J and Mézard M 1997 *Spin-Glasses and Random Fields* (Singapore: World Scientific)
[40] Cugliandolo L F, Kurchan J and Peliti L 1997 *Phys. Rev.* E **55** 3898
[41] Kurchan J 2001 *Jamming and Rheology: Constrained Dynamics on Microscopic and Macroscopic Scales* ed A Liu and S R Nagel (New York: Taylor and Francis)
[42] Monasson R 1995 *Phys. Rev. Lett.* **75** 2847
[43] Franz S and Virasoro M A 2000 *J. Phys. A: Math. Gen.* **33** 891
[44] Edwards S F 1994 *Granular Matter* ed A Mehta (Berlin: Springer)
[45] Barrat A, Kurchan J, Loreto V and Sellitto M 2000 *Phys. Rev. Lett.* **85** 5034
Barrat A, Kurchan J, Loreto V and Sellitto M 2001 *Phys. Rev.* E **63** 051301
[46] Green H S 1952 *The Molecular Theory of Fluids* (Amsterdam: North-Holland)
[47] Yvon J 1969 *Correlations and Entropy in Classical Statistical Mechanics* (Oxford: Pergamon)
[48] Sellitto M 2001 *Phys. Rev.* E **63** 060301
[49] Levin Y, Arenzon J J and Sellitto M 2001 *Europhys. Lett.* **55** 767
[50] Franz S, Mulet R and Parisi G 2002 *Phys. Rev.* E **65** 021506
[51] Sellitto M 2002 *Phys. Rev.* E **65** 020101